Bioelectronic Recordings of Cardiomyocytes with Accumulation Mode Electrolyte Gated Organic Field Effect Transistors

Adrica Kyndiah [a], Francesca Leonardi [b], Carolina Tarantino [c], Tobias Cramer [d], Ruben Millan-Solsona [a,e], Elena Garreta [c], Núria Montserrat [c,f], Marta Mas-Torrent [b], Gabriel Gomila [a,e]*

[a] *Nanoscale Bioelectrical Characterization Group, Institute for Bioengineering of Catalonia (IBEC), The Barcelona Institute of Science and Technology (BIST), Carrer Baldiri i Reixac 11-15, 08028 Barcelona, Spain*

[b] *Institut de Ciència de Materials de Barcelona (ICMAB-CSIC) and Networking Research Centre on Bioengineering Biomaterials and Nanomedicine (CIBER-BBN), Campus UAB Cerdanyola del Vallès, 08193 Barcelona, Spain*

[c] *Pluripotency for Organ regeneration Group, Institute for Bioengineering of Catalonia (IBEC), The Barcelona Institute of Science and Technology (BIST), Carrer Baldiri i Reixac 11-15, 08028 Barcelona, Spain, Centro de Investigación Biomédica en Red en Bioingeniería, Biomateriales y Nanomedicina, Madrid, Spain (CIBER-BBN)*

[d] *Department of Physics and Astronomy, University of Bologna, Viale Berti Pichat 6/2, 40127 Bologna, Italy*

[e] *Departament d'Enginyeria Electrònica i Biomèdica, Universitat de Barcelona, C/ Martí i Franqués 1, 08028 Barcelona, Spain*

[f] *Catalan Institution for Research and Advanced Studies (ICREA), Barcelona, Spain*

* Corresponding author at: Institute for Bioengineering of Catalonia (IBEC), Carrer Baldiri i Reixac 11-15, 08028 Barcelona, Spain
E-mail address: akyndiah@ibecbarcelona.eu

Abstract

Organic Electronic Materials offer an untapped potential for novel tools for low-invasive electrophysiological recording and stimulation devices. Such materials combine semiconducting properties with tailored surface chemistry, elastic mechanical properties and chemical stability in water. In this work, we investigated solution processed Electrolyte Gated Organic Field Effect Transistors (EGOFETs) based on a small molecule semiconductor. We demonstrate that EGOFETs based on a blend of soluble organic semiconductor 2,8-Difluoro-5,11-bis(triethylsilylethynyl)anthradithiophene (diF-TES-ADT) combined with an insulating polymer show excellent sensitivity and long-term recording under electrophysiological applications. Our devices can stably record the extracellular potential of human pluripotent

stem cell derived cardiomyocyte cells (hPSCs-CMs) for several weeks. In addition, cytotoxicity tests of pharmaceutical drugs, such as Norepinephrine and Verapamil was achieved with excellent sensitivity. This work demonstrates that organic transistors based on organic blends are excellent bioelectronics transducer for extracellular electrical recording of excitable cells and tissues thus providing a valid alternative to electrochemical transistors.

Keywords

Bioelectronics, Organic field effect transistors, Organic electronics, Cardiac cells, Organic semiconducting blend

1. Introduction

Measuring the extracellular potential of electrically active cells and tissues in a non-invasive manner is of great interest for developing implantable devices, neuroprothesis (Maya-Vetencourt et al., 2017), brain-computer interfaces (Van De Burgt et al., 2018), artificial synapstors (Desbief et al., 2016, 2015) and *in vitro* drug screening or cytotoxicity tests. The electrical activity of an organ, tissue or cell gives relevant information about its functionality or dysfunctionality, and it can also be used to monitor its functional response to pharmaceutical drugs. Non-invasive recording can be achieved by placing an electrode or a device such as a transistor at the vicinity of the organ/tissue or a cell. When using electrodes, such as the traditional Microelectrode Array Systems (MEAs), the quality of the electrical measurement depends on the interface of the electrode with the tissue or cell. Low impedance electrodes are desirable for high quality recording with MEAs and this can be achieved by increasing the area of the recording electrode thus having the expense of spatial resolution. Alternatively the impedance can be minimized in MEAs by coating the microelectrodes with organic conducting polymers (Inacio et al., 2017; Khodagholy et al., 2011; Sessolo et al., 2013) or nanostructured metallic coatings. Currently available methods in the market also include patch clamp that employs a pipette tip sealed to the cell membrane that can measure the potential between the membrane and the electrode which is then amplified externally. Although this technique is useful to get information at the single cell level, it is labour intensive and invasive as it often leads to cell death due to the rupture of the cell membrane. Another method to measure extracellular potential variations is the light-addressable potentiometric sensor (LAPS) whose detection is based on the coupling of photocurrents to ionic current fluctuations produced by bioelectric activity of cells (Liu et al., 2007). Field Effect Transistor-based platforms, on the other hand, represent an excellent alternative due to their intrinsic signal amplification and scaling down possibilities (Ingebrandt et al., 2001; Khodagholy et al., 2013). Apart from the device layout, the nature of

the interface between the material and the biological system seems to be pivotal for the conversion of biological signals, characterized by an ionic nature, into electronic ones, which rules the mechanism of transduction. There have been many reports in the field of bioelectronics where biosensors, including transistors are based on different types of materials such as inorganic or organic materials, 2D material such as graphene or nanowire transistors (Hess et al., 2011; Zhang and Lieber, 2016). While on the one hand inorganic-based transistors offer advanced signal amplification due to their superior electrical performance as compared to organic transistors, and nanowire FETs offer better sensitivity and the possibility to scale down the device, on the other hand, their mechanical properties, instability when operated in direct contact with water electrochemical environments and the difficulty in chemical modification and fabrication of inorganic devices constitute serious drawbacks.

To address these issues, organic bioelectronic devices have come into the picture. The main advantage of using organic transistors is the mechanical property, surface chemistry and morphology of organic materials can be tuned *ad hoc* in order to reduce invasiveness on the biological tissues (Rivnay et al., 2014; Simon et al., 2016). In addition, organic devices can easily be processed using solution processing techniques avoiding complex fabrication processes and offering the possibility to work on a variety of substrates, such as flexible or resorbable substrates (Campana et al., 2014). Organic based transistors have been employed for extracellular recording by exploiting the electrolyte as a gate of the transistor. Amongst them, Organic Electrochemical Transistor OECTs (Rivnay et al., 2018) and Electrolyte Gated Organic Field Effect Transistors EGOFETs (T. Cramer et al., 2013; Tobias Cramer et al., 2013) are the most documented devices. These devices differ among them basically on the nature of the active material employed. Commonly used material for OECTs is the conducting polymer poly(3,4-ethylenedioxythiophene) doped with poly(styrene sulfonate) (PEDOT:PSS) which works in depletion mode. The functionality of OECTs is governed by injection of cations (depletion mode) or anions (accumulation mode) from the electrolyte that results in the change of the doping state of the material thus modulating the bulk conductivity of the organic semiconductor channel. Due to the coupling between ionic and electronic charges within the entire volume of the channel, OECTs normally have a higher transconductance compared to EGOFETs, but at the expense of higher current densities and power consumption during operation. OECTs have a response time which are relatively slow due to ion diffusion in the bulk material. EGOFETs on the other hand, are considered to be

impermeable to ions and their functionality is governed by the formation of the electrical double layer at the interface between the electrolyte and the semiconductor (Fahlman et al., 2019). Although at amorphous regions of the organic semiconductor ion penetration cannot be completely excluded, (Giridharagopal et al., 2017) a high crystalline film normally ensures the electrostatic accumulation of charge carriers due to the formation of electrical double layer at the electrolyte/semiconductor interface.

Here, we show that the recently proposed solution processed EGOFETs consisting of an organic blend of the bench-mark soluble small molecule 2,8-difluoro-5,11-bis(triethylsilylethynyl)anthradithiophene (diF-TES-ADT) and an insulating polymer polystyrene (PS) enables to overcome previous limitations of EGOFETs and open the way to its application for bioelectric recordings (Zhang et al., 2016). The strategy of using the organic blend of an organic semiconductor with PS has been shown to promote material processability and also leads to thin films with an enhanced crystallinity and environmental stability (Del Pozo et al., 2016; Temiño et al., 2016). With the aim to employ these organic blend EGOFETs as bioelectronic recording platform, here we demonstrate the capability of EGOFETs based on a solution processed organic material diF-TES-ADT blended with polystyrene PS to record the extracellular action potentials of human Pluripotent Stem Cells derived cardiomyocyte cells (hPSCs CMs). hPSCs CMs represent a promising and powerful tool in cardiac biology for cardiac disease modelling. This cellular platform was recently exploited for the generation of hPSCs-derived cardiac grafts to screen the effect of drugs on human atrial and ventricular electrophysiology (Garreta et al., 2016). We demonstrate that the electrical activity of the cultured cells plated on an EGOFET array can be recorded for several days with extreme stability. Compared to the state of the art EGOFETs reported so far, our device shows a remarkable stability in physiological conditions with a charge carrier mobility decrease almost negligible (less than 1 order of magnitude) and with a shift in threshold voltage below 0.1V. In addition, we also show the possibility to perform cytotoxicity tests of different pharmaceutical drugs, such as norepinephrine and verapamil, on these devices. We note that the use of EGOFETs to monitor the electrical activity of hPSCs derived cardiomyocytes can offer an excellent *in vitro* platform to cardiac disease modelling, cardiac toxicology and regeneration.

2. Materials and methods

2.1 Device fabrication

A semi-transparent biocompatible Kapton foil (Kapton® HN from DuPont, 75 μm thick) was used as substrate for our devices; source and drain (S/D) electrodes were defined by maskless photolithography (MicroWriter ML™ Laser Lithography System) and a metal layer of Cr/Au (5 nm/40 nm) was subsequently evaporated (System Auto 360 from BOC Edwards). The channel width (W) and length (L) were 19680 μm and 30 μm (namely having a geometrical ratio W/L = 656), respectively. Prior to the deposition of the organic semiconductor, the substrates were cleaned in ultrasonic bath with acetone and isopropanol for 15 min respectively and afterward ozone-treated for 25 min. S/D electrodes were subsequently modified by immersing the device in a 15 mM pentafluorothiophenol (PFBT) solution in isopropanol for 15 minutes. A blend composed of diF-TES ADT and polystyrene (PS) was chosen as semiconductor material. The two components were mixed in a 4:1 ratio, and then dissolved in chlorobenzene reaching a final concentration of 2 wt%. The blend solution was kept on a hot-plate at 105 °C for 1 h to ensure the complete dissolution of the starting materials. Thin film deposition was realized through Bar-Assisted Meniscus Shearing (BAMS) technique by means of a home-adapted bar coater working at fixed speed of 1 cm s^{-1} and at a fixed plate temperature of 105 °C as reported earlier (Leonardi et al., 2016; Zhang et al., 2016). All the above-mentioned processes were realized under ambient conditions. Prior to cell seeding the devices were coated with a thin matrigel layer (BD Biosciences) by drop casting. We verified that the addition of the matrigel layer does not affects severely the device response and it greatly facilitates cell adhesion.

2.2 Cell Culture

Single cell suspension of human Pluripotent Stem Cells (hPSCs) were seeded onto matrigel (BD Biosciences) pre-coated cell culture dishes at a density of 125,000 cells per cm^2 in mTeSR medium (StemCell Technologies), supplemented with 5 μM ROCK inhibitor (Y-27632, Sigma-Aldrich). Cells were then maintained in mTeSR with ROCK inhibitor for 24 h and in mTeSR only, for one more day. Differentiation was initiated by treatment with 12 μM CHIR99021 (Selleck) in RPMI (Invitrogen) supplemented with B27 minus insulin (Life Technologies), 2 mM L-glutamine, 0.1 mM 2-mercaptoethanol, nonessential amino acids and penicillin-streptomycin (RPMI/B27-insulin medium) for 24 h (day 0 to day 1). On day 1, the inhibitor was removed by washing with RPMI medium and then maintained in RPMI/B27-insulin medium for two more days. On day 3, cells were treated with 5 μM Wnt inhibitor IWP4 (Stemgent) in RPMI/B27-insulin medium and cultured without medium change for 48 h. On day 5, cells were washed once with RPMI to eliminate the inhibitor and maintained in

RPMI (Invitrogen) supplemented with B27 (Life Technologies), 2 mM L-glutamine, 0.1 mM 2-mercaptoethanol, nonessential amino acids and penicillin-streptomycin (RPMI/B27 medium). From day 5, cells were maintained in RPMI/B27 medium with medium change every 2 days.

On day 14, beating monolayers were obtained. For video recording, hPSC-derived cardiomyocyte monolayers were imaged at 37ºC in RPMI/B27 medium using a Leica MC170HD camera connected to a DM IL LED microscope (Leica). Starting from day 20, clusters of 300-500 beating cells (seeding density is determined based on the surface area to be occupied by the beating cell) were detached from the plate, seeded on the top of device transistors, previously coated with matrigel, and further maintained in RPMI/B27 medium during the course of the recording experiment. The medium was changed every two days during the course of the experiment.

2.3 Immunocytochemistry

hPSC-derived cardiomyocyte monolayers were fixed with 2% paraformaldehyde (Aname) for 20 min at room temperature. Next, samples were washed twice with PBS and further blocked and permeabilized for 1 h at room temperature with Tris-buffered saline (TBS) containing 0.5% Triton X100 (Sigma) and 6% donkey serum (Millipore). Samples were then incubated overnight at 4 °C with primary antibodies. The following primary antibodies were used: Myosin Heavy Chain (MYH6, GTX20015, 1:100, GeneTex); GATA 4 binding 4 (GATA4, sc9053, 1:25, Santa Cruz Biotechnology); NKX2.5 (sc8697, 1:25, Santa Cruz Biotechnology); Troponnin T (TNN, MS-295-P1ABX, 1:500, Thermo Scientific). After the incubation with primary antibodies, samples were washed three times with TBS containing 0.1% Triton X100 (Sigma) and 6% donkey serum (Millipore) and further incubated for 2 h at room temperature with fluorescent-conjugated secondary antibodies (Alexa Fluor (A) 488-, Cy3- or A647-; 1:200). After three rinses with PBS, samples were counterstained with 4,6-diamidino-2-phenylindole (DAPI; Life Technologies, 1:5000) for 30 min for the detection of nuclei. Samples were then mounted using Fluoromount-G (Southern Biotech). Image acquisition was carried out using a SP5 (Leica) confocal microscope.

2.4 Drugs tested

Norepinephrine Bitartrate salt ($C_8H_{11}NO_3 \cdot C_4H_6O_6$) and Verapamil hydrochloride 5-[*N*-(3,4-Dimethoxyphenylethyl)methylamino]-2-(3,4-dimethoxyphenyl)-2-isopropylvaleronitrile

hydrochloride were both purchased from Sigma Aldrich. Norepinephrine was dissolved in cell medium while Verapamil was dissolved in Ethanol.

2.5 EGOFET characterization

All electrical device characterizations were performed by employing a cell culture media mTeSR, which is the cell culture medium commonly used for human embryonic stem cells, as working electrolyte and a Pt wire (Ø = 0.5 mm) as the gate electrode. The measurements were all carried out inside the incubator under the standard conditions of 37°C temperature, 80% humidity and 5% CO_2. Agilent B2912A was used as a source measuring unit for the electrical recording of the transistor. Prior to the recording experiment, typical transistor characterization of Source-Drain current (I_{SD}) versus Source-Gate voltage (V_{GS}) was carried out. For recording the extracellular potentials of cardiac cells, the transistor was operated at V_{GS}= - 0.7 V and V_{DS}=-0.5 V, and the current I_{SD} was monitored over time. The signals were recorded continuously for a time span of 1000 seconds. Recordings were repeated for at least 3 times a day. The frequency response of the transistor was measured by using a function generator 33220A Function Waveform Generator (Keysight) coupled to the Agilent B2912A. A sinusoidal wave oscillation of 10mV was applied to V_{GS}, with the device set at V_{GS} = -0.7 V and V_{DS} = -0.5 V.

3. Results and Discussion

3.1 Electrical characterisation of the EGOFET in electrophysiological condition

The schematic diagram of the EGOFET with a cluster of cells plated on the channel of the transistor is depicted in **Figure 1**(a), while figure 1(b) shows a picture of the actual device and figure 1(c) a zoom in image with hPSC derived cardiomyocytes plated on top of the transistors area. The substrate of the device consists of a flexible biocompatible kapton foil onto which interdigitated gold electrodes 30 nm thick were deposited. The organic semiconductor diF-TES-ADT blended with polystyrene PS was coated onto the substrate using the Bar-Assisted Meniscus Shearing technique (BAMS) as reported earlier (Leonardi et al., 2016; Zhang et al., 2016). In addition, the device used here was coated with matrigel to favour the adhesion of the cells to the semiconductor layer. We verified that the presence of the matrigel layer does not degrade appreciably the performance of the device **(Figure S1)**. The electrical characteristics of this EGOFET, before cell plating, is depicted in figure 1d. In this case, cell medium mTeSR was used as working electrolyte. A Source-Gate Voltage V_{GS}

is applied between the gate electrode (Pt wire) immersed in the liquid (see figure 1(b)) and the source electrode, at fixed source-drain voltage, V_{DS}. The application of a gate potential promotes the formation of a double layer at the interface between the electrolyte and the organic semiconductor. Since our active organic material forming the channel of the transistor is a p-type semiconductor, the application of a negative potential results in the accumulation of positive charges (holes) on the semiconductor. When a potential is applied across the Source and Drain electrodes V_{DS}, charges move across the channel giving rise to the source drain current I_{DS}, whose intensity depends on the source gate voltage, V_{GS} as shown in figure 1(d).

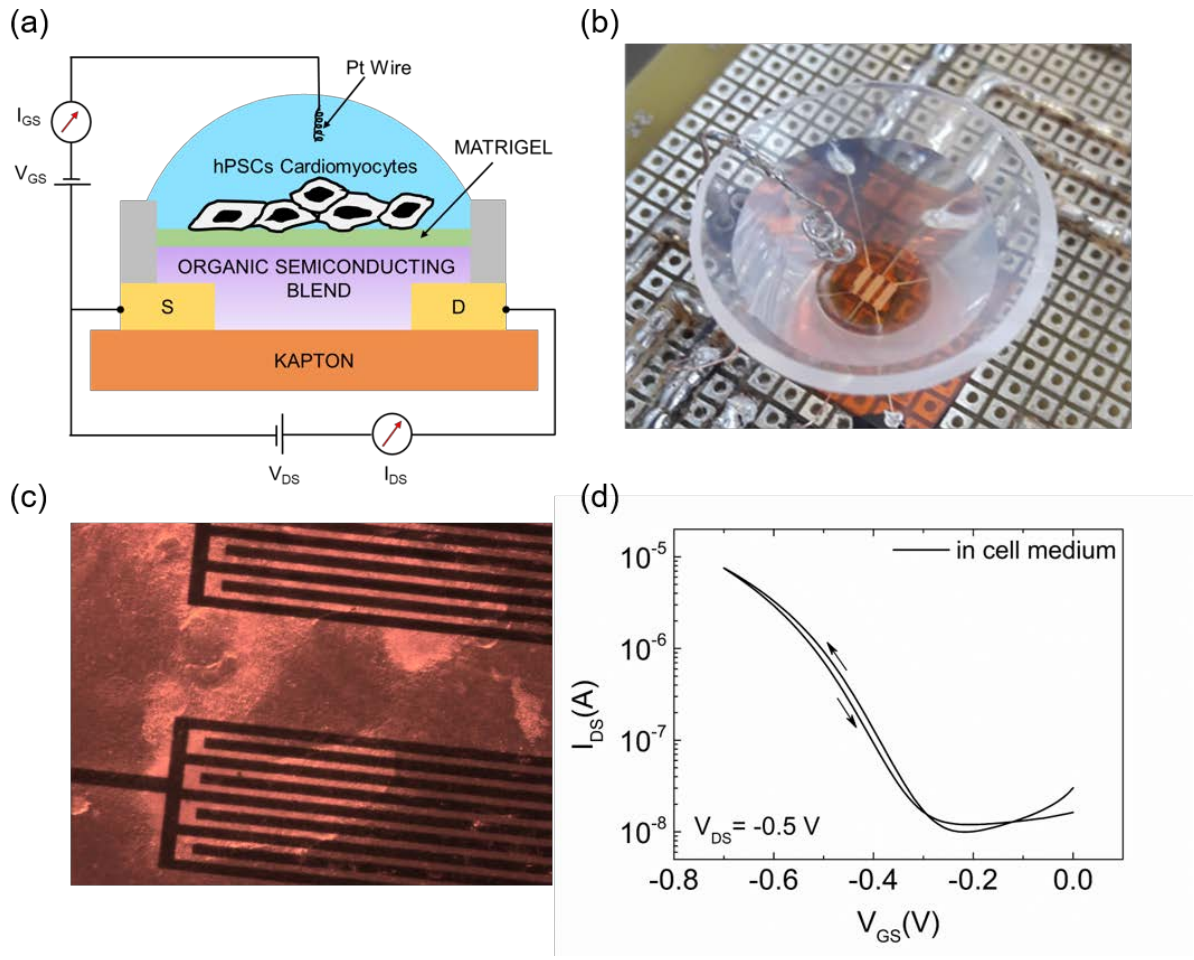

Figure 1. (a) Schematic diagram of the EGOFET coupled to hPSCs-CMs grown as a cluster of cells. (b) Photograph of the experimental setup for extracellular recording. (c) Optical microscopy image of hPSCs-CMs on the EGOFET (d) Typical Source-Drain current I_{DS} characteristics versus Gate-Source Voltage V_{GS} of the transistor operated in cell medium, for V_{DS}=-0.5V. Arrows indicate the forward and reverse scan of the IV curve.

For extracellular recordings, the main EGOFETs parameters that must be taken into account are the potentiometric sensitivity, the time response and, most importantly, the stability during the course of the recording experiment. In order to determine the potentiometric sensitivity, we applied a constant gate and drain voltage (V_{GS} = -0.7V and V_{DS}=-0.5V) and monitored the changes in source drain current ΔI_{SD} in response to the application of voltage pulses to the gate of amplitude ΔV_{GS}, as shown in **Figure 2**a. We have verified that the transistor is sensitive to gate voltages changes down to 20μV. This implies that the device can transduce extracellular potentials at least down to 20 μV. To gain further insight into the performance of the EGOFETs, a frequency response characterization of the device was carried out by measuring the transconductance of the transistor. Fixing V_{DS} at -0.5 V and V_{GS} at -0.7 V, a 10mV peak-to-peak sine wave oscillation was applied on the V_{GS}. A cut-off frequency of ≈ 3 KHz is obtained for our EGOFETs (Figure 2b). Finally, the stability of the devices in physiological condition was investigated by monitoring the characteristics of the EGOFET with cell medium as an electrolyte inside a cell incubator periodically. Figure 2 (c) is a control experiment without cells where we study the stability of our EGOFETs as a function of time in physiological condition. The devices were operated using the cell medium as an electrolyte and were placed inside the incubator under the conditions of temperature of 37 °C, humidity 90%, 5% CO_2. This study represents a key point of our work because organic electronic devices are in general considered very sensitive to environmental factors. Factors such as temperature, humidity and a poor electrical instability in “complex” electrolyte such as the cell medium can hinder their application in bioelectronics. However, one of the main points of this work relies on the demonstration of the superior robustness of our EGOFETs that is proved with the control experiment reported in Figure 2 (c) where no electrical failures are observed after 3 weeks in electrophysiological condition. In order to further demonstrate the robustness of our device, two important figures of merit, i.e. transconductance g_m and threshold voltage V_{th}, has been plotted (see supplementary figure S5).

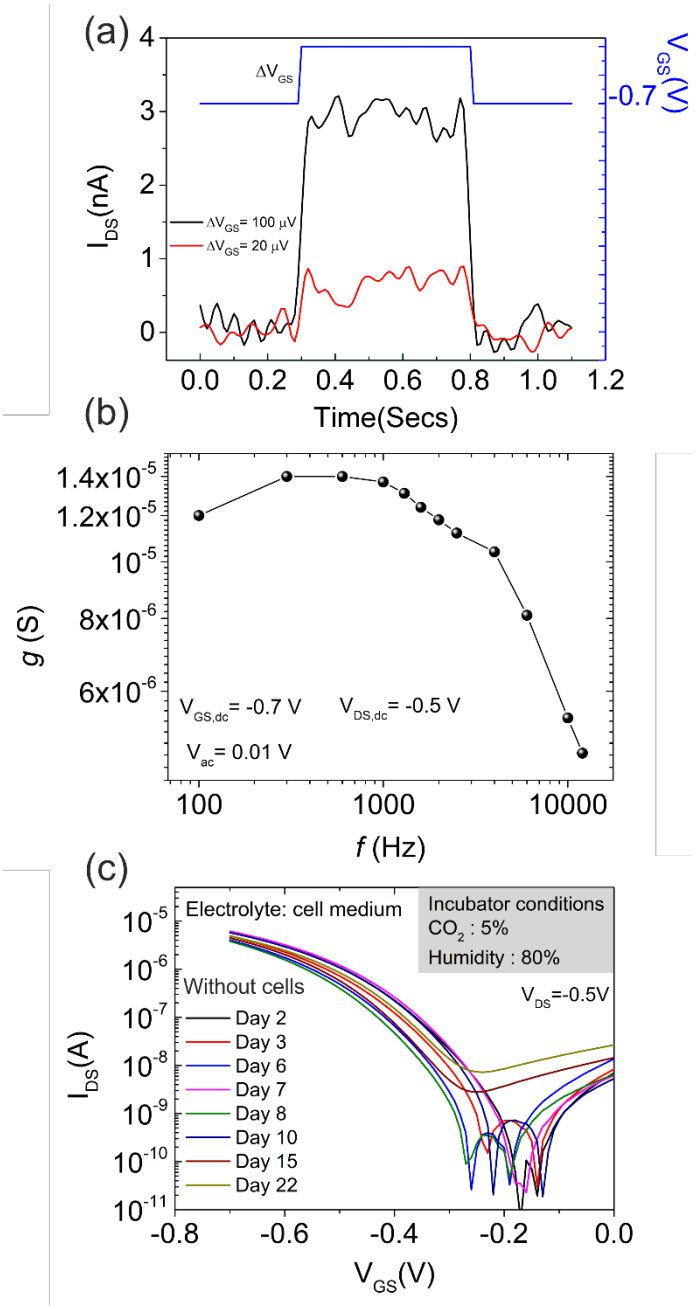

Figure 2 (a) Potentiometric sensitivity of the EGOFETs used in this study. Black and red lines correspond to the modulation of I_{DS} due to V_{GS} square pulses of amplitudes 100 µV and 20 µV, respectively. Measurements are recorded in cell medium at V_{DS} = −0.5 V. (b) Frequency response of the transconductance of the EGOFETs at V_{GS} = −0.7 V and V_{DS} =-0.5 V. (c) Source-Drain current I_{DS} characteristics versus Gate-Source Voltage V_{GS} of the transistor operated in cell medium taken for several days. The EGOFET was kept with the electrolyte in the incubator for several weeks.

3.2: Electrical recording of cardiomyocyte cells

To demonstrate the capability of these devices to record extracellular bioelectronic signals, hPSCs-CMs that exhibit spontaneous beating phenomena (**Supplementary information**

video S1) were plated on the EGOFETs (**Supplementary information video S2)**. hPSCs-CMs were grown as monolayer cell cultures and further transferred on the device upon differentiation (from day 12 during the protocol of differentiation) (Garreta et al., 2016). hPSC-CMs monolayers showed the expression of major proteins associated with cardiac muscle contraction including Troponin T (TNN) and Myosin Heavy Chain (MYH6), as well as nuclear transcription factors related to cardiac fate such as NK2 Homeobox 5 (NKX2.5) and GATA binding protein 4 (GATA4) as determined by immunofluorescence analysis (**Supplementary Figure S2 (a) and S2 (b)**). For recording the cardiac action potential, EGOFETs were operated at V_{GS}=-0.7 V and V_{DS}=-0.5 V, and the Source Drain current I_{SD} was monitored as a function of time. It normally took 5-7 days for the cluster of cells to adequately couple to the EGOFET channel to generate high electrical signals as also observed in previous reports (Gu et al., 2019). After a good coupling was achieved and a regular beating of the plated cells was observed (see video in the supplementary information) spikes on the I_{SD} were easily detected (**figure 3**(a), black trace). The recordings were taken continuously for at least 1000 seconds, with a signal to noise ratio of the recordings between 3-4 which is comparable to the ones measured using OECTs (Liang et al., 2018; Susloparova et al., 2016; Yao et al., 2015). A fast Fourier transform of the time trace (figure 3(b)) showed that the frequency of the spikes was ~ 0.65 Hz, which nicely agrees with the frequency of contractions observed with the optical microscope. Taking into account the transconductance of the EGOFET, g_m=20 nA/mV, the gate voltage variation caused by the extracellular potential spike was calculated to be $\Delta V_{GS}=\Delta I_{SD}/g_m$= 40µV, well within the limit of detection of our device, as demonstrated earlier in figure 2(a). We remark that each device contains three transistors (see figures 1(c) and S3), and current spikes were only observed for transistors with cells positioned directly on top of the channel (dark pink trace figure 3(a) and supplementary information, **Figure S3**).

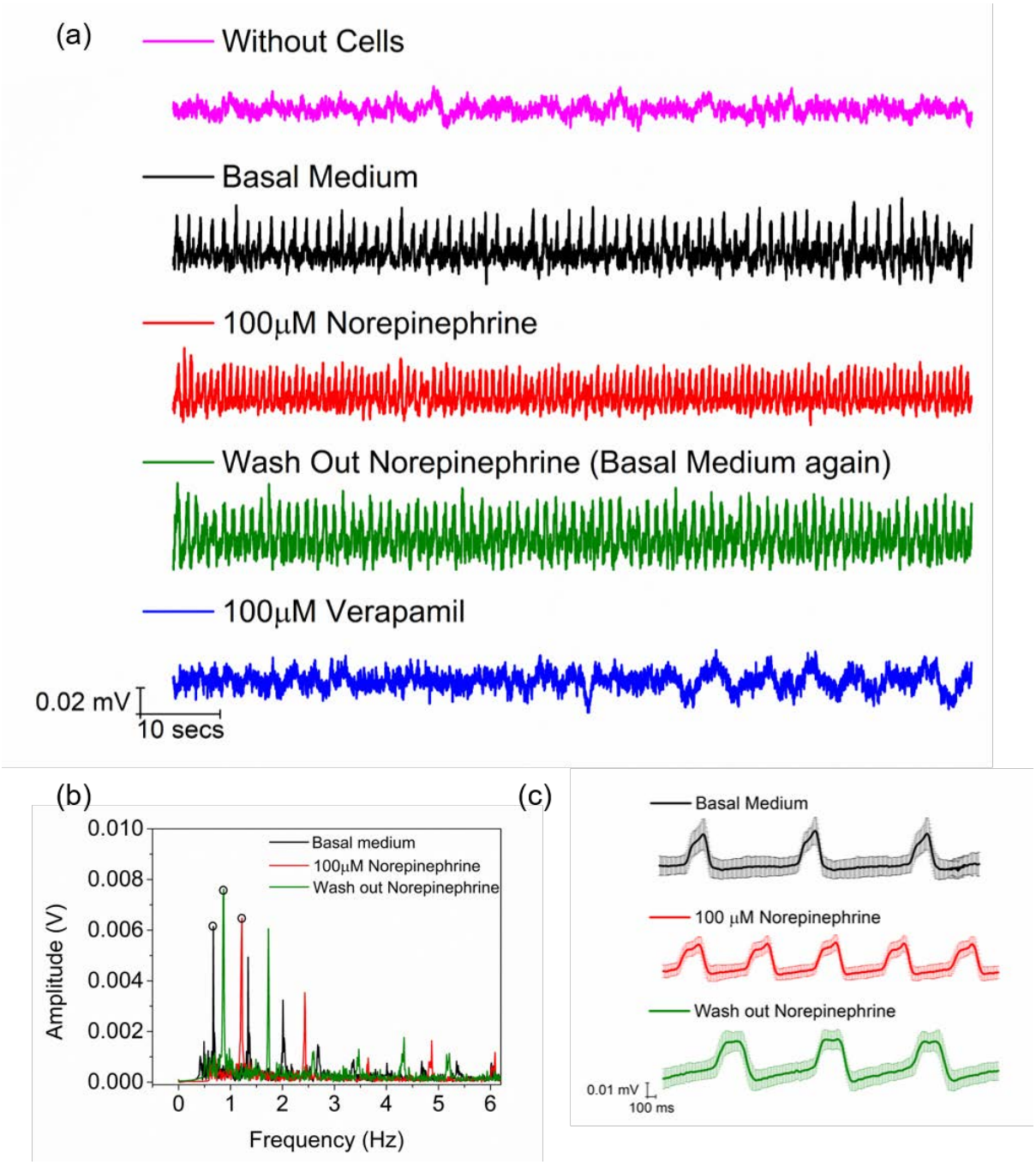

Figure 3 (a). Representative electrical recordings performed with the EGOFET device on hPSC derived cardiac cells under different conditions. The time traces are presented as equivalent gate voltage variations obtained from source drain current variations as $\Delta V_{GS}=\Delta I_{SD}/g_m$. The dark pink curve depicts the electrical recording of an EGOEFT in the absence of cells. The black curve corresponds to basal medium; the red curve to basal medium with the addition of a 100µM of Norepinephrine; the green curve to basal medium again after the drug is wash out; and the blue curve to basal medium when 100µM of Verapamil drug is added. (b) Fast Fourier transform of the time traces shown in (a) for the different conditions. The circle shows the peak of the first harmonic used to identify the characteristic frequency of the time traces. (c) Representative shape of the extracellular potentials corresponding to the average of n = 40 spikes.

3.3: Pharmacology test

In order to take advantage of this platform we further assessed the effect of two well-known chronotropic agents, namely norepinephrine and verapamil. First, to modulate the frequency of the beating rate of the cardiac cells, 100 µM of norepinephrine were added. Norepinephrine is a widely used cardio stimulant agent known to increase the beating rate of cardiac cells. The frequency of the spikes recorded after the addition of the drug indeed increased up to 1.3 Hz (figures 3(a) and 3(b), red lines), which is twice faster than the frequency observed in basal cell medium. This observation is in accordance with previous investigation on the effect of Norepinephrine on hPSC-CMs (Huang et al., 2017). After the electrical recording, norepinephrine drug was washed out. The cells were rinsed with PBS solution and the basal cell medium was added again. The frequency of the electrical signal recorded following the washing out of the drug recovered back to 0.8 Hz, which is closer to the pre-drug recording (figures 3(a) and 3(b) green lines). We also took advantage of verapamil, a drug acting as blocker of calcium channels. Towards this end, 100 µM of Verapamil was added to the cell culture. Accordingly, no electrical spikes higher than the instrumental noise level were detected (figures 3(a) and 3(b), blue lines).

Importantly, we were able to show that the shape of the recorded spikes was quite reproducible. In this regard, Figure 3(c) shows the average shape of the spikes obtained from the average of 40 spikes for the different conditions examined. The shapes do not display the expected shape of extracellular potentials corresponding to single cardiomyocytes. The reason can be due to the complex 3D nature of the cluster of cells and its coupling with the EGOFETs. Further work becomes necessary to clarify this point.

3.4 : Stability of the EGOFETs in physiological condition

One of the more relevant results obtained with these EGOFETs refers to its remarkable stability in physiological operation as seen in figure 2 (c). It is well known that organic transistors generally show instabilities in the presence of humidity, temperature and water (Bobbert et al., 2012). However, the performance of the transistors used in the present study the performance of the transistors used in the present study seem to be unaltered. **Figure 4**a shows the I-V (source-drain current versus source-gate voltage) curves which were recorded during the whole experimental duration (10 days) to check the lifetime of the device. I-V curves are figures of merit of a field effect transistor, which include information about the quality of the device. Such characterization is essential for the complete understanding of the electrical behaviour of the device in presence of cultured cells and it is a good indicator of its capability of transduction.

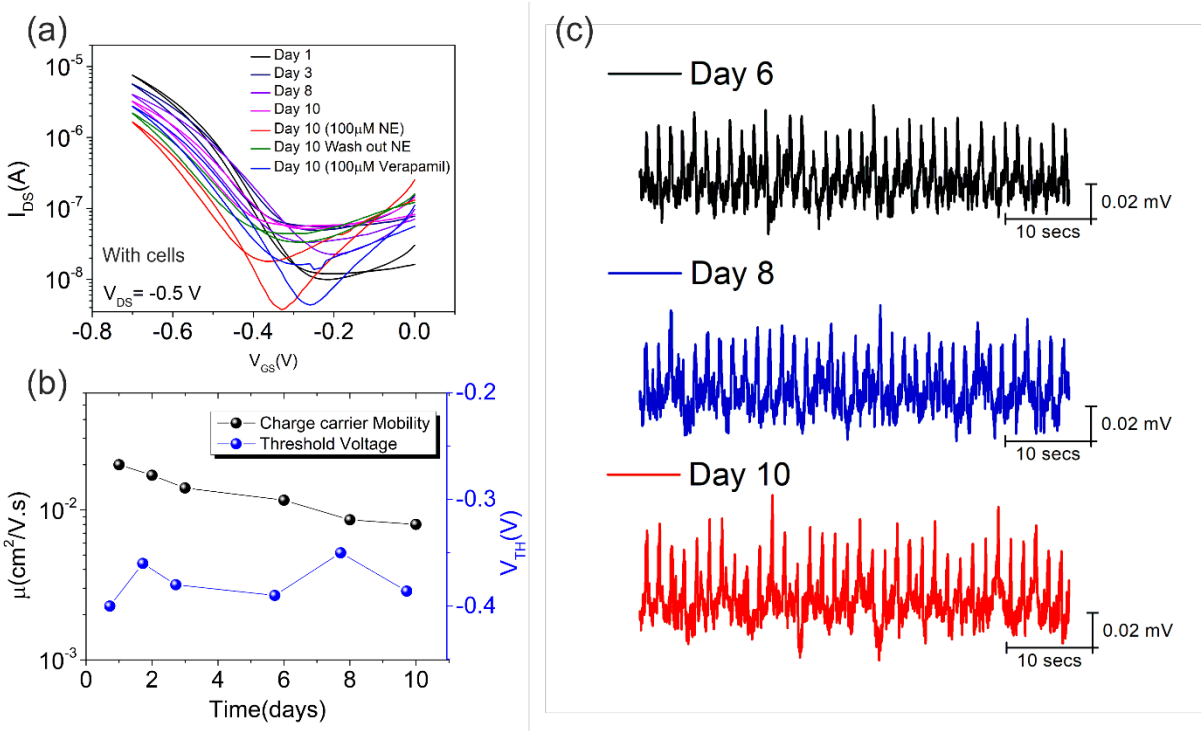

Figure 4. (a) Typical transistor IV curves recorded during the whole study. The legend describes the day when the IV curve is recorded, and which drug has been added to the cell medium. Day 1 corresponds to the first day when the cell is seeded on the device. (b) Charge carrier mobility µ as a function of time in days on the left y axis (black square markers) and Threshold Voltage V_{TH} as a function of time in days on the right blue axis x (square blues markers). (c) Representative electrical recording taken on different days, showing the stability of the device over several days.

As can be seen, after 10 days with cells, the transconductance of the transistor does not decrease significantly. The superior performance of these EGOFETs is attributed to the high crystallinity of the active thin film which has been deposited through a solution shearing technique, i.e. BAMS, starting from a precursor ink of diF-TES-ADT and polystyrene (Del Pozo et al., 2016; Leonardi et al., 2016). Furthermore, in the present case, the I-V characteristics are also good indicators of the status of the transistor in response to drugs such as norepinephrine and verapamil. The EGOFETs stability is reflected in the fact that the charge carrier mobility decrease is almost negligible and the shift in threshold is below 0.1V during days of operation (see figure 4(b) that depicts the change in µ and V_{th} as a function of days). The charge carrier mobility µ and threshold voltage V_{th} is extracted using the formula

$$I_{SD,sat} = \frac{W}{L} C_{DL}\, \mu\, (V_{GS} - V_{th})^2$$

where W and L are the width and length of the channel and C_{DL} is the capacitance of the double layer. We illustrate the stability of the devices by showing also recorded traces corresponding to days 6, 8 and 10. As can been seen, the signal to noise ratio did not decrease

as a function of days. The outstanding stability of these devices allow us not only to carry out extracellular recording for over 10 days but also to study the effect of drugs on the bioelectrical activity of the cardiac cells. We have further checked the electrical performance of an operating transistor in physiological conditions for a month's time and, as can be seen from Figure 2c, the EGOFET still shows excellent performance without any relevant drop in the current.

We have demonstrated that EGOFETs based on a blend of the organic semiconductor diF-TES-ADT with polystyrene can provide stable extracellular electric potential recordings on electrically excitable cells such as hPSC-CMs. As compared to previous works using EGOFETs, our device shows a much higher stability when operated in physiological conditions. The stability of our devices is attributed to the high crystallinity and smoothness of the films deposited by the shearing technique BAMS (Campos et al., 2018; Pérez-Rodríguez et al., 2018). The stability of these EGOFETs is reflected in the minimal change of the transconductance of the transistor during operation in physiological conditions over time. As an application of these EGOFETs we have considered the study of the electrical activity on cardiomyocyte-like cells derived from hPSCs under different experimental conditions. Our experimental setting resulted in further culture of hPSCs-CMs beating monolayers as cluster of cells forming stable interfaces with these organic devices. Thus, this study proves feasibility when envisioning the use of EGOFETs for the performance of long-time studies using electrically excitable cells. It is well accepted that the use of hPSCs and their differentiated cell types (as cardiomyocytes) offer an unprecedented platform for the study of human disease. In this regard the possibility to monitor the electrophysiological activity of hPSC-CMs represents a straightforward approach in further applications related to cardiac drug toxicity and cardiac disease modelling taking advantage for the combination of this cells together with EGOFETs. Of note, the long-term stability of the blend based EGOFET-hPSCs cardiac cell platform would offer a plethora of opportunities to further analyse all these questions and increase our armamentarium of technologies when envisioning hPSCs-CMs as major cell sources for understanding cardiac cell biology, cardiac development or disease.

4. Conclusions

To conclude, this work proves unambiguously that small molecule based EGOFETs can be used as a recording platform to measure the bioelectrical response of excitable cells. Its operation in accumulation mode with relatively lower charge densities and power

consumption makes it a valid alternative to the commonly used PEDOT PSS based OECTs. EGOFETs employed in this work are based on an organic blend of diF-TES-ADT and Polystyrene which can be easily processing by a printing technique. The functionality of these devices remains unaltered when an extracellular matrix such as Matrigel commonly used for attaching cells is coated on top of the transistor, and when the devices is maintained in physiological conditions over weeks. Their ability to sense potential changes down to 20 µV at timescales of few millivolt makes them promising candidate for sensing bioelectrical signals. In this work, we record the bioelectrical signal of spontaneously beating embryonic cardiomyocyte cells which couple to the transistor channel. Cardiac action potential of 40 µV are recorded at a frequency of 0.65 Hz corresponding to the frequency of the beating / contraction of the cardiac cells. The effect of pharmaceutical drugs such as Norepinephrine and Verapamil on the electrical activity of the cardiac cells was also successfully demonstrated by using these devices. The stability of these EGOFETs when operated in physiological environment outstands the state of the art EGOFET. The stability, high sensitivity and simple architecture of these devices could be exploited in several directions, including the realization of *in vitro* fundamental studies on electrical active cell differentiation and maturation or the development of implantable devices to monitor bioelectric signals *in vivo*.

Acknowledgments

This work has been partially supported by the BEST Postdoctoral Programme funded by the European Commission under Horizon 2020's Marie Curie Sklodowska-Curie Actions COFUND scheme (GA 712754) and the Severo Ochoa programme of the Spanish Ministry of Science and Competitiveness (SEV-2014-0425 (2015-2019) and SEV-2015-0496) and the BORGES project (Marie Curie Skłodowska European Training Network (MSCA-ITN-ETN)) under the GrantAgreement (GA) No: 813863. G. G. acknowledges support from an ICREA Academia award from the Generalitat de Catalunya and from the Agencia Estatal de Investigación (Nanoelectrophys project, TEC2016-79156-P). The authors also thank the DGI (Spain) project FANCY CTQ2016-80030-R, the Generalitat de Catalunya (2017-SGR-918) and the Networking Research Center on Bioengineering, Biomaterials, and Nanomedicine (CIBER-BBN). Dr. F. Leonardi gratefully acknowledges the "Juan de la Cierva" programme. The authors thank S. Ricci for her help on the samples preparation. This work has received funding from the European Research Council (ERC) under the European Union's Horizon 2020 research and innovation programme (StG-2014-640525_REGMAMKID to C.T. and

N.M.). NM has received funding from the Spanish Ministry of Economy and Competitiveness/FEDER (SAF2015-72617-EXP and SAF2017-89782-), the Generalitat de Catalunya and CERCA programme (2017 SGR 1306), Asociación Española contra el Cáncer (LABAE16006 to N.M.) and by CardioCel (TerCel, Instituto de Salud Carlos III). IBEC is the recipient of a Severo Ochoa Award of Excellence from MINECO.

References

Bobbert, P.A., Sharma, A., Mathijssen, S.G.J., Kemerink, M., De Leeuw, D.M., 2012. Adv. Mater. 24, 1146–1158.

Campana, A., Cramer, T., Simon, D.T., Berggren, M., Biscarini, F., 2014. Adv. Mater. 26, 3874–3878.

Campos, A., Riera-Galindo, S., Puigdollers, J., Mas-Torrent, M., 2018. ACS Appl. Mater. Interfaces 10, 15952–15961.

Cramer, T., Campana, A., Leonardi, F., Casalini, S., Kyndiah, A., Murgia, M., Biscarini, F., 2013. J. Mater. Chem. B 1, 3728–3741.

Cramer, T., Chelli, B., Murgia, M., Barbalinardo, M., Bystrenova, E., de Leeuw, D.M., Biscarini, F., 2013. Phys. Chem. Chem. Phys. 15, 3897.

Del Pozo, F.G., Fabiano, S., Pfattner, R., Georgakopoulos, S., Galindo, S., Liu, X., Braun, S., Fahlman, M., Veciana, J., Rovira, C., Crispin, X., Berggren, M., Mas-Torrent, M., 2016. Adv. Funct. Mater. 26, 2379–2386.

Desbief, S., di Lauro, M., Casalini, S., Guerin, D., Tortorella, S., Barbalinardo, M., Kyndiah, A., Murgia, M., Cramer, T., Biscarini, F., Vuillaume, D., 2016. Org. Electron. 38, 21–28.

Desbief, S., Kyndiah, A., Guérin, D., Gentili, D., Murgia, M., Lenfant, S., Alibart, F., Cramer, T., Biscarini, F., Vuillaume, D., 2015. Org. Electron. 21, 47–53.

Fahlman, M., Fabiano, S., Gueskine, V., Simon, D., Berggren, M., Crispin, X., 2019. Nat. Rev. 4, 627–650.

Garreta, E., de Oñate, L., Fernández-Santos, M.E., Oria, R., Tarantino, C., Climent, A.M., Marco, A., Samitier, M., Martínez, E., Valls-Margarit, M., Matesanz, R., Taylor, D.A., Fernández-Avilés, F., Izpisua Belmonte, J.C., Montserrat, N., 2016. Biomaterials 98,

64–78.

Giridharagopal, R., Flagg, L.., Harrison, J.., Ziffer, M.., Onorato, J., Luscombe, C.., Ginger, D.., 2017. Nat. Mater. 16, 1–6.

Gu, X., Yeung, S.Y., Chadda, A., Poon, E.N.Y., Boheler, K.R., Hsing, I.M., 2019. Adv. Biosyst. 3, 1800248.

Hess, L.H., Jansen, M., Maybeck, V., Hauf, M. V., Seifert, M., Stutzmann, M., Sharp, I.D., Offenhäusser, A., Garrido, J.A., 2011. Adv. Mater. 23, 5045–5049.

Huang, C., Booth, R.H., O'Hara, T.J., Wheeler, E.K., Liao, R., Kulp, K.S., Soscia, D.A., Enright, H.A., Creek, C.J., Qian, F., Ivanovskaya, A.N., Belle, A.M., Lin, Y.-D., Lightstone, F.C., 2017. Lab Chip 17, 1732–1739.

Inacio, P.M.C., Mestre, A.L.G., De Medeiros, M.D.C.R., Asgarifar, S., Elamine, Y., Canudo, J., Santos, J.M.A., Braganca, J., Morgado, J., Biscarini, F., Gomes, H.L., 2017. IEEE Sens. J. 17, 3961–3966.

Ingebrandt, S., Yeung, C.K., Krause, M., Offenhäusser, A., 2001. Biosens. Bioelectron. 16, 565–570.

Khodagholy, D., Doublet, T., Gurfinkel, M., Quilichini, P., Ismailova, E., Leleux, P., Herve, T., Sanaur, S., Bernard, C., Malliaras, G.G., 2011. Adv. Mater. 23, 268–272.

Khodagholy, D., Doublet, T., Quilichini, P., Gurfinkel, M., Leleux, P., Ghestem, A., Ismailova, E., Hervé, T., Sanaur, S., Bernard, C., Malliaras, G.G., 2013. Nat. Commun. 4, 1575.

Leonardi, F., Casalini, S., Zhang, Q., Galindo, S., Gutiérrez, D., Mas-Torrent, M., 2016. Adv. Mater. 28, 10311–10316.

Liang, Y., Ernst, M., Brings, F., Kireev, D., Maybeck, V., Offenhäusser, A., Mayer, D., 2018. Adv. Healthc. Mater. 7, 1800304.

Liu, Q., Cai, H., Xu, Y., Xiao, L., Yang, M., Wang, P., 2007. Biosens. Bioelectron. 22, 3224–3229.

Maya-Vetencourt, J.F., Ghezzi, D., Antognazza, M.R., Colombo, E., Mete, M., Feyen, P., Desii, A., Buschiazzo, A., Di Paolo, M., Di Marco, S., Ticconi, F., Emionite, L., Shmal, D., Marini, C., Donelli, I., Freddi, G., MacCarone, R., Bisti, S., Sambuceti, G., Pertile,

G., Lanzani, G., Benfenati, F., 2017. Nat. Mater. 16, 681–689.

Pérez-Rodríguez, A., Temiño, I., Ocal, C., Mas-Torrent, M., Barrena, E., 2018. ACS Appl. Mater. Interfaces 10, 7296–7303.

Rivnay, J., Inal, S., Salleo, A., Owens, R.M., Berggren, M., Malliaras, G.G., 2018. Nat. Rev. Mater. 3, 17086.

Rivnay, J., Owens, R.M., Malliaras, G.G., 2014. Chem. Mater. 26, 679–685.

Sessolo, M., Khodagholy, D., Rivnay, J., Maddalena, F., Gleyzes, M., Steidl, E., Buisson, B., Malliaras, G.G., 2013. Adv. Mater. 25, 2135–2139.

Simon, D.T., Gabrielsson, E.O., Tybrandt, K., Berggren, M., 2016. Chem. Rev. 116, 13009–13041.

Susloparova, A., Lu, X., Hempel, F., Ingebrandt, S., Munief, W., Law, J.K.-Y., Nguyen, T.C., Vu, X.T., Pachauri, V., 2016. Biosens. Bioelectron. 93, 132–138.

Temiño, I., Del Pozo, F.G., Ajayakumar, M.R., Galindo, S., Puigdollers, J., Mas-Torrent, M., 2016. Adv. Mater. Technol. 1, 1600090.

Van De Burgt, Y., Melianas, A., Keene, S.T., Malliaras, G., Salleo, A., 2018. Nat. Electron. 1, 386–397.

Yao, C., Li, Q., Guo, J., Yan, F., Hsing, I.M., 2015. Adv. Healthc. Mater. 4, 528–533.

Zhang, A., Lieber, C.M., 2016. Chem. Rev. 116, 215–257.

Zhang, Q., Leonardi, F., Casalini, S., Temiño, I., Mas-Torrent, M., 2016. Sci. Rep. 6, 1–10.